

NUMERICAL MODELING OF THE SOLIDIFICATION PROCESS WITH CONSIDERATION OF SHRINKAGE CAVITIES FORMATION AND THE INFLUENCE OF SOLID PHASE CONTENT ON THE FEEDING OF THE CASTING

Ewa Węgrzyn-Skrzypczak¹, Tomasz Skrzypczak²

¹ *Department of Mathematics, Czestochowa University of Technology
Czestochowa, Poland*

² *Department of Mechanics and Fundamentals of Machine Design, Czestochowa University
of Technology, Czestochowa, Poland*

ewa.wegrzyn-skrzypczak@pcz.pl, tomasz.skrzypczak@pcz.pl

Received: 27 February 2023; Accepted: 12 April 2023

Abstract. The paper focuses on the numerical modeling of the three-dimensional solidification process of steel using the finite element method (FEM). The model includes and discusses the formation of shrinkage cavities and the influence of the solid phase content on the feeding of the casting through the riser. The analysis assumed a critical value of the solid phase content, at which the transport of liquid phase from the riser to the casting is interrupted. The results of numerical simulation are presented to investigate the influence of this factor on the final quality of the casting. The model neglects the fluid motion in the liquid and solid-liquid regions and replaces the influence of the mold with appropriate boundary conditions.

MSC 2010: 65M60, 68U20

Keywords: solidification process, finite element method, shrinkage cavities, computational mechanics

1. Introduction

Reduction of the volume of the alloy during the solidification process leads to the formation of micro- and macroscopic voids dispersed throughout the casting. Material shrinkage caused by temperature decrease is observed in both liquid and solid phases due to density changes dependent on temperature. Shrinkage before and after solidification has a significantly smaller impact on the formation of defects than the volume loss associated with the liquid-to-solid phase transition. This is the main cause of macroscopic defects in castings. The total volume of the casting decreases during three consecutive stages of the process – cooling of the casting in the liquid state, solidification, cooling of the solidified casting. The first stage

begins after filling the mold with liquid metal and ends at the beginning of solidification. At this stage, the upper surface of the liquid metal in the raiser is observed to sink. This work omits this stage and focuses only on the solidification stage, which occurs between the liquidus and solidus temperatures. The shrinkage of the casting during this stage is mainly controlled by the liquid-to-solid transformation. The liquid phase has a greater volume than the solid phase due to its lower density. The transformation of the liquid into a solid leads to the formation of shrinkage voids in the casting. Depending on its shape and cooling conditions, macroscopic voids can be distributed differently in the final product. The shrinkage of the solidified material in the last stage of the casting forming process is caused by the shrinkage of the material in the solid state resulting from cooling and is also omitted in this work. The most common macroscopic defects are cone-shaped open voids observed at the top of the raiser and closed voids located deeper in the solidifying system [1-3]. Numerical models of the formation of shrinkage defects are widely discussed in the literature [4-12]. Fundamental information on the formation of shrinkage cavities in the context of casting solidification can be found in books [4, 5]. The study [6] addresses the problem of predicting the distribution of defects in a simple-shaped casting. With the increase in computer computational power, the formation of shrinkage cavities in three-dimensional areas has been modeled [7-12], using proprietary software [7] as well as commercial software [8-12], where the formation of porosities [9] and additional factors such as macrosegregation of components [8, 10, 11] were taken into account. Commercial software is dominant in the literature, and self-developed computational solvers are less frequently described. The presented article is devoted to numerical modeling of the solidification process and formation of shrinkage cavities during which the casting is fed with liquid phase from the riser. The considerations assume that the feeding process is stopped at a certain critical value of the solid phase fraction in the area between the raiser and the casting. The discussed model allows for dynamical controlling the feeding process depending on the structure of the solid-liquid phase between the raiser and the casting. Simulations were performed with the use of proprietary software. Previous works were based on a simplified model in which the feeding was interrupted when the solid phase fraction was greater than 0.

2. Problem description

In Figure 1, a solidifying casting with marked characteristic zones is presented. The interior of the casting is occupied by the solidification zone Ω_S , the mushy zone Ω_M filled with a mixture of liquid and solid phases, the liquid areas Ω_{L1} , Ω_{L2} , and the shrinkage cavity zones Ω_{SC1} , Ω_{SC2} . The process of the formation of the open shrinkage cavity Ω_{SC1} begins earlier than Ω_{SC2} because it is enforced by gravity. The second shrinkage cavity, located deeper, is formed only when the supplying of the liquid in the lower part of the system is stopped. This happens when a solid phase appears in the connector between the upper and lower parts of the system

with a participation exceeding a certain critical value. From that moment on, with the passage of time, both shrinkage cavities evolve until the liquid areas in the analyzed system disappear. Of course, this is a particular case chosen, because depending on the shape of the solidifying system and the cooling conditions, one or more macroscopic defects caused by material shrinkage may finally appear. In addition to the characteristic areas, the external boundary of the analyzed area, Γ_{ext} , and the symmetry plane of the casting, Γ_{sym} , are also marked in Figure 1. It is assumed that the system is symmetrical in order to limit the numerical analysis only to half of the system in further proceedings.

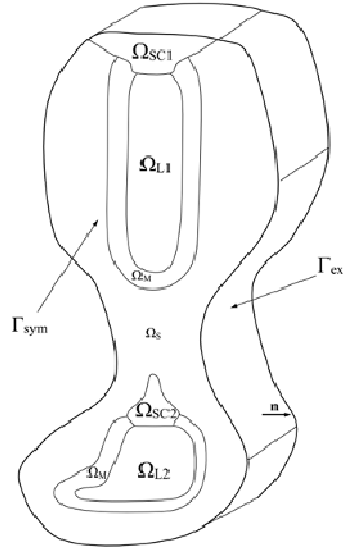


Fig. 1. Solidifying area with marked characteristic zones

The fundamental mathematical framework for describing the problem involves the transient heat transfer partial differential equation (1), along with the corresponding initial (2) and boundary conditions (3)-(4):

$$\nabla \cdot (\lambda \nabla T) = c \rho \frac{\partial T}{\partial t} \quad (1)$$

$$T(x, y, z, t = 0) = T_0 \quad (2)$$

$$(x, y, z) \in \Gamma_{sym} : -\mathbf{n} \cdot \lambda \nabla T = 0 \quad (3)$$

$$(x, y, z) \in \Gamma_{ext} : -\mathbf{n} \cdot \lambda \nabla T = \alpha (T - T_\infty) \quad (4)$$

In this context, λ [$\text{J s}^{-1} \text{m}^{-1} \text{K}^{-1}$] represents thermal conductivity, T [K] refers to the temperature, c [$\text{J kg}^{-1} \text{K}^{-1}$] is the effective specific heat parameter used to describe heat release during solidification, ρ [kg m^{-3}] refers to density, t [s] represents

time, \mathbf{n} is the normal vector to the external boundary Γ_{ext} , α [$\text{J s}^{-1} \text{m}^{-2} \text{K}^{-1}$] is the heat transfer coefficient, T_0 [K] represents the initial temperature distribution and T_∞ [K] represents the temperature of the external medium (such as a mould or air), ∇ is the Nabla operator.

The density ρ in the liquid, solid, and mushy regions and thermal diffusion coefficient λ are determined by computing their respective average values using the following simple formulas:

$$\begin{aligned}\rho &= f_S \rho_S + f_L \rho_L \\ \lambda &= f_S \lambda_S + f_L \lambda_L\end{aligned}\quad (5)$$

The parameters f_L and f_S [-] are dimensionless and represent the fractions of liquid and solid, respectively. These parameters are determined as functions of temperature:

$$f_S = \frac{T_L - T}{T_L - T_S}, \quad f_L = 1 - f_S \quad (6)$$

The symbol T_L [K] represents the liquidus temperature, while T_S [K] represents the solidus temperature.

The effective specific heat can be expressed in the following manner [13]:

$$\begin{aligned}T < T_S : & \quad c = c_S \\ T_S \leq T \leq T_L : & \quad c = \frac{c_L + c_S}{2} + \frac{L}{T_L - T_S} \\ T > T_L : & \quad c = c_L\end{aligned}\quad (7)$$

In the above equation, c_S and c_L [$\text{J kg}^{-1} \text{K}^{-1}$] represent the specific heat coefficients for the solid and liquid fractions, respectively, while L [J kg^{-1}] denotes the latent heat of solidification.

As shown in Equation (7), there is a significant increase in the specific heat within the mushy zone due to the heat released during solidification. The model presented allows for the presence of separate liquid, solid, liquid-solid, and gaseous regions, and it ensures that the gas phase does not mix with any other phases. Furthermore, the material properties of air are taken into account in the model for shrinkage cavities.

3. Numerical model

The formulation of the finite element method (FEM) for the described numerical model utilizes Equation (1) supplemented with initial and boundary conditions (2)-(4), for which the criterion of weighted residuals has been applied:

$$\int_{\Omega} w \left[-c\rho \frac{\partial T}{\partial t} + \nabla \cdot (\lambda \nabla T) \right] d\Omega = 0 \quad (8)$$

In the above equation, the symbol w represents the test function dependent on spatial coordinates, and Ω denotes the total volume of the casting. The standard Galerkin formulation is employed to derive a set of spatially discretized equations. For a single finite element (e), the following equation can be obtained in the similar way as in [14]:

$$(c\rho)^{(e)} \iint_{\Omega^{(e)}} \mathbf{N}^T \mathbf{N} d\Omega \dot{\mathbf{T}} + \lambda^{(e)} \iint_{\Omega^{(e)}} (\mathbf{D}_x^T \mathbf{D}_x + \mathbf{D}_y^T \mathbf{D}_y + \mathbf{D}_z^T \mathbf{D}_z) d\Omega \mathbf{T} = - \oint_{\Gamma^{(e)}} \mathbf{N} q d\Gamma \quad (9)$$

The equation involves the shape functions of the finite element in \mathbf{N} , the spatial derivatives of shape functions with respect to x , y , and z , denoted by \mathbf{D}_x , \mathbf{D}_y , and \mathbf{D}_z , respectively, and \mathbf{T} , which contains the nodal values of temperature and its time derivatives $\dot{\mathbf{T}}$. The boundary heat flux is represented by q .

To compute the temperature distribution, the backward Euler method is utilized for the operation of time discretization, resulting in the following scheme:

$$\left((\Delta t)^{-1} \mathbf{M} + \mathbf{K} \right) \mathbf{T}^{j+1} = \mathbf{B} + (\Delta t)^{-1} \mathbf{M} \mathbf{T}^j \quad (10)$$

In the above equation, \mathbf{K} and \mathbf{M} refer to global conductivity and heat capacity matrices, respectively. \mathbf{B} is the vector that holds the boundary conditions. The time step is represented by Δt [s], while j indicates the current time level.

3.1. The numerical process of formation of shrinkage cavities

The process of forming shrinkage cavities involves the use of finite element mesh nodes. Initially, the total volume of the solidifying area is distributed among the mesh nodes. Subsequently, nodal volumes can be determined using the finite element mesh structure. A nodal volume represents the volume associated with a particular nodal point and is calculated as the sum of the fractional volumes of the finite elements connected to that nodal point [15].

At the beginning of the solidification process, the entire area is filled with liquid phase. Each of the nodes, in addition to its assigned volume, has a defined state – liquid (L), solid-liquid (SL), solid (S), or gas (air) (A). Initially, all nodes are in a liquid state (L). As time passes, the solid phase grows in the area and the volume of liquid regions gradually shrinks. Depending on the shape of the casting and cooling conditions, two or more separated liquid regions may form. Complete separation occurs when a solid body or a solid-liquid material with a sufficiently high solid fraction is present between the liquid regions, which means that there is no possibility of gravitational flow of the liquid phase from one liquid region to another.

Partial separation occurs when a mixture of solid and liquid phases with a relatively low solid fraction is present between the liquid regions. In this case, it is assumed that the liquid regions are still connected because the flow of liquid between them is possible. Therefore, an important element of the method used for forming shrinkage cavities is to correctly identify the liquid regions depending on their location in the casting and the state of the material between them. In [16], a similar but simplified model was used, in which complete separation of the liquid regions was assumed when any small amount of solid phase appeared between them. In this study, it was assumed that the semi-solid zone consists of spherical grains growing in the liquid matrix (Fig. 2). It was assumed that the flow of liquid between the grains is possible until neighboring grains come into contact with each other.

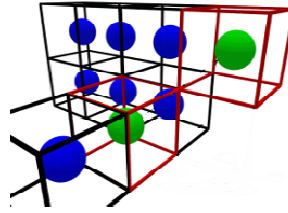


Fig. 2. Structure of the mushy zone (spherical grains in cubical cells)

With this assumption, the critical value of the solid phase fraction at which fluid flow occurs in the solid-liquid zone is $f_{skr} = 0.52$:

$$f_{skr} = \frac{V_{grain}}{V_{cell}} = \frac{\frac{4}{3}\pi\left(\frac{a}{2}\right)^3}{a^3} = \frac{1}{6}\pi \cong 0.52 \quad (11)$$

The algorithm of shrinkage cavity growth can be presented in the following stages at each time step:

1. Based on the computed temperature field in the current time step and the temperature field from the previous step, the increment of the solid phase is calculated. In the case where there is only one liquid region in the casting or the liquid regions are not completely separated from each other, the global increment of the solid phase is calculated. In the case of two or more completely separated liquid regions, the increment of the solid phase must be calculated separately for each of them.
2. After calculating the increment of the solid phase, the material shrinkage is computed by multiplying the volume of the solid phase by the shrinkage coefficient S_h .
3. The calculated volumetric loss of material is assigned to the highest located nodes (L) in the corresponding liquid regions. At the same time, the state of these nodes changes from (L) to (A). In this way, the number of nodes (A) gradually increases, forming one or more shrinkage cavities.

This process is repeated at each time step until the disappearance of (L) nodes in the casting. Of course, this is not the end of the solidification process, since there are still nodes in the (SL) state. However, introducing the assumption that only (L) nodes can change state to (A) marks the end of the shrinkage cavity growth process.

4. Example of calculations

The geometry of the system (casting along with the riser) was prepared in the GMSH program [17]. The object has dimensions of 0.45x0.65x0.5 m, with only half of the entire system shown in Figure 3 due to symmetry with respect to the plane parallel to the xy -plane.

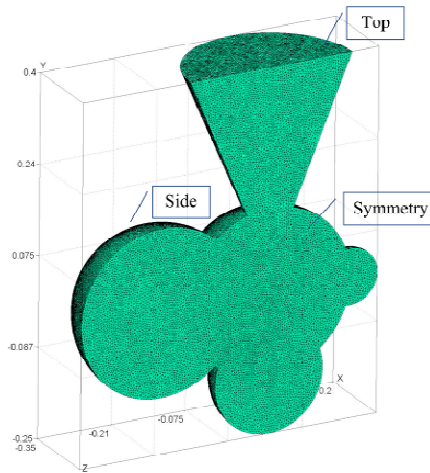


Fig. 3. Casting along with the riser divided into finite elements

The geometry has been divided into 627332 tetrahedral finite elements to facilitate the analysis. The entire mesh comprises 122301 computation points or nodes, which allow for accurate modeling of the casting process. Figure 3 depicts the boundaries of the area, which consist of three surfaces: the upper surface of the riser "Top," the lateral surface that represents the actual contact area between the casting and the mold "Side," and the plane of symmetry "Symmetry." The material properties used in the calculations are listed in Table 1.

The following boundary conditions were adopted:

- On the "Top" surface: $\alpha = 20 \text{ J s}^{-1} \text{ m}^{-2} \text{ K}^{-1}$, $T_{\infty} = 300 \text{ K}$.
- On the "Side" surface: $\alpha = 200 \text{ J s}^{-1} \text{ m}^{-2} \text{ K}^{-1}$, $T_{\infty} = 300 \text{ K}$.
- On the "Symmetry" surface: $q = 0 \text{ J s}^{-1} \text{ m}^{-2}$.

The initial temperature was assumed to be $T_0 = 1833 \text{ K}$. The computational process was carried out with a time step of $\Delta t = 0.5 \text{ s}$ until the complete solidification of the casting.

Table 1. Material properties used in calculations

Material property	Solid phase	Liquid phase	Air
λ [$\text{J s}^{-1} \text{m}^{-1} \text{K}^{-1}$]	35.0	23.0	0.03
P [kg m^{-3}]	7800.0	6915.0	1.0
c [$\text{J kg}^{-1} \text{K}^{-1}$]	644.0	837.0	1008.2
T_L [K]	1774.0		–
T_S [K]	1718		–
L [J kg^{-1}]	270000		–
S_h [–]	0.05		–
f_{skr} [–]	0.52		

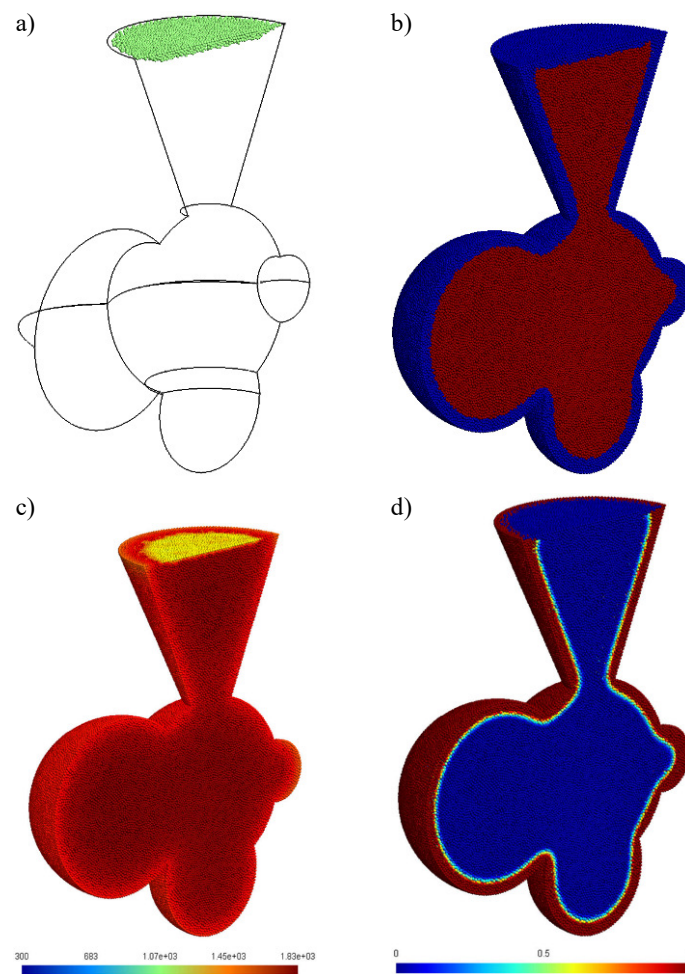


Fig. 4. Shrinkage cavity (a), identified regions with liquid phase flow (b), temperature field (c), and solid phase fraction (d) after 200 s

After 200 s from the start of the cooling process, an open-top shrinkage cavity is formed at the top of the casting (Fig. 4a). Deeper, no shrinkage cavities are observed due to the supply of liquid phase from the riser. This is visible in Figure 4b where the red color indicates the area where liquid flow is possible, while the blue color marks the area where $f_s > f_{skr}$ and also where the space is occupied by air. No distinction was made in the coloring of these areas. The material in the casting is still hot and mostly liquid, with the only significantly cooler region appearing in the forming funnel of the shrinkage cavity (Fig. 4c). The solid phase is observed along the outer boundaries (Fig. 4d). The solid-liquid zone is strongly reduced at this stage due to the rapid growth of the solid phase from the outer edges towards the center of the casting.

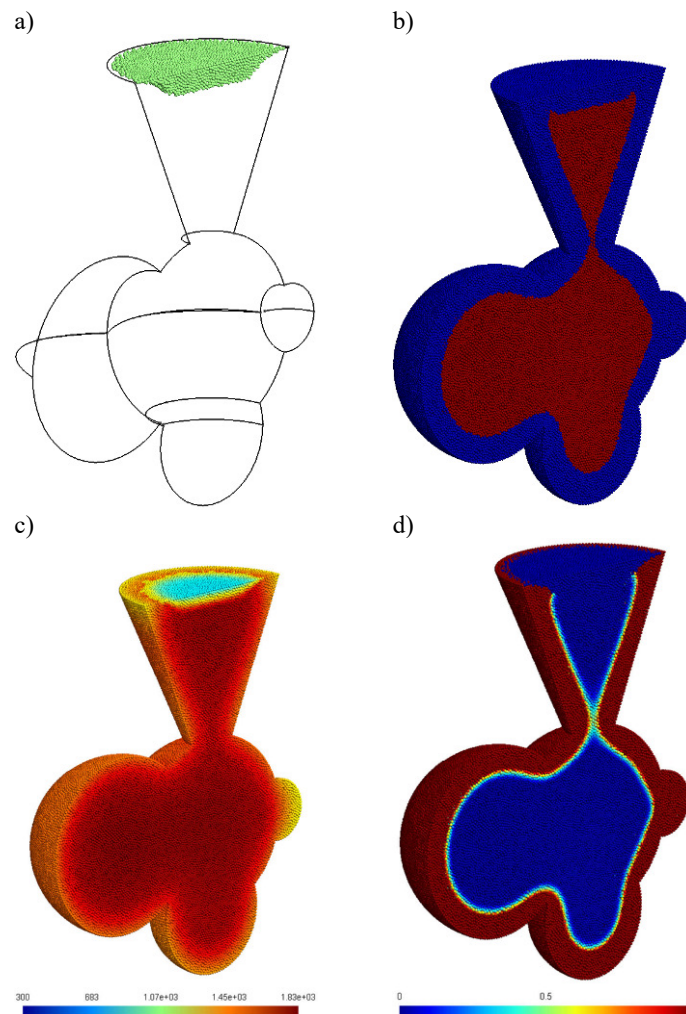


Fig. 5. Shrinkage cavity (a), identified regions with liquid phase flow (b), temperature field (c), and solid phase fraction (d) after 400 s

After 400 s from the start of the process, only one shrinkage cavity is still observed at the top of the casting (Fig. 5a). Figure 5b shows that it is still possible to supply the casting with liquid phase from the riser, as the solid phase fraction at the constriction between these elements did not exceed the critical value of f_{skr} . The temperature field is shown in Figure 5c, while the solid phase fraction is shown in Figure 5d. It is clearly visible that the solid phase is growing at the constriction between the casting and the riser, which will soon interrupt the feeding process.

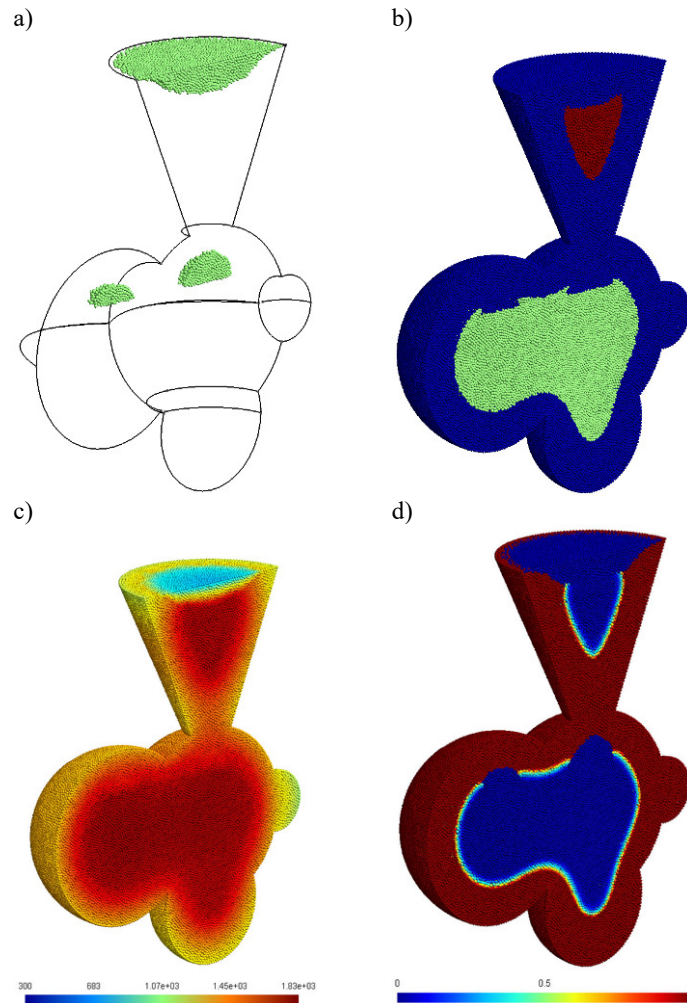


Fig. 6. Shrinkage cavities (a), identified regions with liquid phase flow (b), temperature field (c), and solid phase fraction (d) after 600 s

After 600 s, three shrinkage cavities are visible in the casting, one in the riser and two located deeper (Fig. 6a). In Figure 6b, two separate solidifying zones are

visible (red and green), indicating the interruption of the feeding of the casting by liquid from the riser. Figure 6c shows the temperature field with clear hot spots at the top and bottom. In Figure 6d, the solidified material is also visible at the constriction between the top and bottom parts of the system, as well as the shape of the developing shrinkage cavities. The state after solidification is shown in Figure 7a-b.

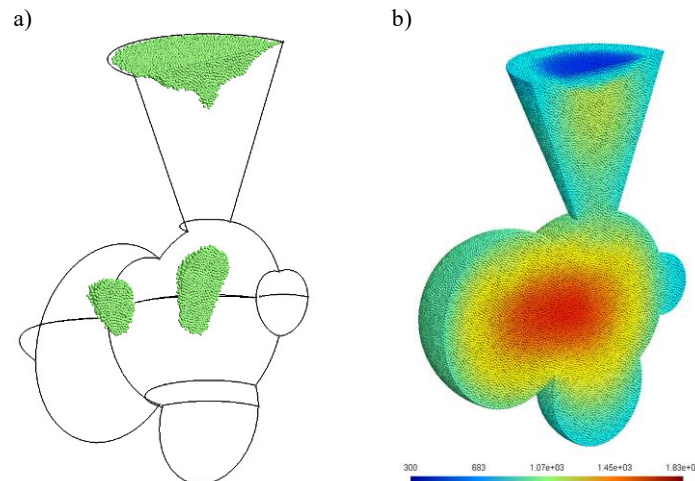


Fig. 7. Shrinkage cavities (a) and the temperature field (b) at the end of solidification process (1380 s)

5. Conclusions

A mathematical and numerical description of the three-dimensional solidification process taking into account the formation of shrinkage cavities has been presented. The results of the performed calculations demonstrate the effectiveness of the utilized mathematical and numerical models and the computer program developed based on them. The described approach is useful for modeling the formation of multiple macroscopic defects caused by material shrinkage during solidification. Depending on the structure of the solid-liquid zone, it is possible to introduce the critical value of the solid phase fraction at which the feeding process of the molten metal from the riser into the casting is terminated. The original computer program based on the finite element method is robust and efficient for complex three-dimensional geometries. It is also free and more flexible than expensive commercial packages. Further work focuses on the experimental validation of the described model and the inclusion of additional phenomena accompanying solidification, such as macrosegregation of impurity elements and analysis of the resulting structures depending on the cooling rate.

References

- [1] Pequet, Ch., Rappaz, M., & Gremaud, M. (2002). Modeling of microporosity, macroporosity, and pipe-shrinkage formation during the solidification of alloys using a mushy-zone refinement method: Applications to aluminum alloys. *Metallurgical and Materials Transactions A*, 33(7), 2095-2106.
- [2] Bellet, M., Jaouen, O., & Poitroult, I. (2005). An ALE-FEM approach to the thermomechanics of solidification processes with application to the prediction of pipe shrinkage. *International Journal of Numerical Methods for Heat and Fluid Flow*, 15(2), 120-142. DOI: 10.1108/0961530510578410.
- [3] Hajkowski, J., Roquet, P., Khamashta, M., Codina, E., & Ignaszak, Z. (2017). Validation tests of prediction modules of shrinkage defects in cast iron sample. *Archives of Foundry Engineering*, 17(1), 57-66. DOI: 10.1515/afe-2017-0011.
- [4] Campbell, J. (2003). *Castings*, (2nd ed.). Oxford: Butterworth-Heinemann.
- [5] Flemings, M.C. (1974). *The Solidification Processing*. New York: Mc Graw-Hill.
- [6] Kim, C.J., & Ro, S.T. (1993). Shrinkage formation during the solidification process in an open rectangular cavity. *Journal of Heat Transfer*, 115(4), 1078-1081. DOI: 10.1115/1.2911369.
- [7] Jabur, A.S., & Kushnaw, F.M. (2017). Casting simulation and prediction of shrinkage cavities. *Journal of Applied & Computational Mathematics*, 6(4), 7. DOI: 10.4172/2168-9679.1000371.
- [8] Ludwig, A., Wu, M., & Kharicha, A. (2016). On the importance of modeling 3D shrinkage cavities for the prediction of macrosegregation in steel ingots. in: *CFD Modeling and Simulation in Materials Processing 2016*, 3-10. DOI: 10.1007/978-3-319-65133-0_1.
- [9] Zhang, C., Bao, Y., Wang, M., & Zhang L. (2016). Shrinkage porosity criterion and its application to a 5.5 ton steel ingot. *Archives of Foundry Engineering*, 16(2), 27-32. DOI: 10.1515/afe-2016-0021.
- [10] Wu, M., Ludwig, A., & Kharicha, A. (2017). A four phase model for the macrosegregation and shrinkage cavity during solidification of steel ingot. *Applied Mathematical Modelling*, 41, 102-120. DOI: 10.1016/j.apm.2016.08.023.
- [11] Xie, M., & Shen, H. (2020). Multiphase model for the prediction of shrinkage cavity, inclusion and macrosegregation in a 36-ton steel ingot. *Frontiers in Materials*, 7, 13. DOI: 10.3389/fmats.2020.577290.
- [12] Zheng, K., Lin, Y., Chen, W., & Liu, L. (2020). Numerical simulation and optimization of casting process of copper alloy water-meter shell. *Advances in Mechanical Engineering*, 12(5), 1-12. DOI: 10.1177/1687814020923450.
- [13] Mochnacki, B., & Suchy, J.S. (1993). *Modeling and Simulation of Solidification of Castings*. Warsaw: PWN.
- [14] Skrzypczak, T., Węgrzyn-Skrzypczak, E., & Sowa, L. (2018). Numerical modeling of solidification process taking into account the effect of air gap. *Applied Mathematics and Computation*, 321, 768-779. DOI: 10.1016/j.amc.2017.11.023.
- [15] Liu, X.L. (2000). Isothermal flow simulation of liquid composite molding. *Composites: Part A*, 31, 1295-1302.
- [16] Skrzypczak, T., Sowa, L., & Węgrzyn-Skrzypczak, E. (2020). Numerical model of solidification including formation of multiple shrinkage cavities. *Archives of Foundry Engineering*, 20(1), 37-42. DOI: 10.24425/afe.2020.131280
- [17] Geuzaine, C., & Remacle, J.-F. (2009). Gmsh: a three-dimensional finite element mesh generator with built-in pre- and post-processing facilities. *International Journal for Numerical Methods in Engineering*, 79(11), 1309-1331.